Available online at www.sciencedirect.com
SCIENCE DIRECT®
Thermochimica Acta 423 (2004) 89–97
thermochimica acta
www.elsevier.com/locate/tca

The principle of micro thermal analysis using atomic force microscope

Chunhai Wang*

Veeco Instruments, 112 Robin Hill Road, Santa Barbara, CA 93117, USA

Received 10 July 2003; received in revised form 10 February 2004; accepted 19 April 2004
Available online 19 June 2004

Abstract

A mathematical model for micro thermal analysis is developed based on heat conduction equation. It interprets the principle of micro thermal analysis by relating its signals directly to established parameters of materials, such as thermal conductivity, specific heat etc. Based on the theory, a new instrument is designed employing three components of electrical current to drive a thermal probe. A high frequency component is used to measure probe temperature; a low frequency and a dc component are used for temperature control. Thermal properties of materials are measured by monitoring ac temperature response to a known ac driving power and monitoring dc power consumption for a known dc temperature input. With the new design, thermal information of a sample can be separated from the artifact caused by a measuring probe. Glass transitions of polymers can be easily identified from both dc and ac signals.

Keywords: Micro thermal analysis; Scanning thermal probe microscope; Atomic force microscope; Thermal probe

1. Introduction

Atomic force microscope (AFM) is a powerful tool for imaging micro world down to the size of individual atoms. Its imaging capability includes topography, capacitance, static charge, magnetic and other force modes. Thermal analysis focuses on the measurement of thermal properties, such as temperature, thermal conductivity, heat capacity and phase transition point. AFM had not been used for thermal analysis until 1993 when Majumdar et al. [1] integrated a thermocouple at the tip of an AFM cantilever. The thermocouple was used to measure temperature while normal AFM force feedback maintained the contact between the tip and the sample. In this way, both topography and temperature were mapped. To expand the capability of AFM for thermal analysis, Dinwiddie et al. [2] introduced a technique for measuring thermal conductivity, in which a resistive probe was used as both a heating source and thermometer. The probe was kept at constant temperature. Thermal conductivity was mapped by monitoring power consumption. A further milestone improvement was Hammiche et al.'s introduction of temperature ramping to micro thermal analysis [3]. Hammiche et al's design employeded two probes: a measuring probe and a reference probe. Dc and ac current were applied simultaneously to both probes. Voltage difference between two probes served as the output. This design made it possible to measure phase transitions. Commercial instruments had not been available until 1998. After that, research activities have greatly increased (such as [4–32]). Micro thermal analysis is finding more and more applications in polymer, pharmaceutical and semiconductor science.

Despite of a decade of research, it is still early to say that the technology of micro thermal analysis is mature. In theoretical aspect, researchers are not clear what constitutes ac signals. Ac signals were first interpreted as related to thermal diffusivity. The idea was later dropped. In instrumentation, a more reliable technique for temperature measurement and control is needed in order to improve the sensitivity of thermal analysis. Since the size of a thermal tip is very small, it is very difficult to integrate both a heater and a thermometer on it. A resistive tip is usually used instead, which serves as both a heater and a thermometer. Wheatstone bridge is used accordingly for temperature control. A disadvantage of this technique is that the current for raising the temperature of a probe is not constant. As a result, the voltage drop

* Tel.: +1 805 9672700; fax: +1 805 9677717.
E-mail address: cwang@veeco.com (C. Wang).

0040-6031/$ – see front matter © 2004 Elsevier B.V. All rights reserved.
doi:10.1016/j.tca.2004.04.021

over the probe does not represent the resistance of thermal probe or temperature. Although probe resistance can be measured theoretically by dividing its voltage over its current, available analog divider is too noisy for this application and digital one is usually too slow to follow the fast changing ac temperature. The reality limits the functionality of micro thermal analysis only to the mode of measuring power for known temperature modulation. It is very difficult to implement measuring temperature for known power modulation, although power modulation can be done more accurately as power modulation does not involve thermal dynamics of a probe. 3-ω Method was considered as a possible alternative for measuring ac temperature [32]. However the low sensitivity in measuring the third harmonics offsets the advantage of power modulation, limiting its application.

This paper presents a theory that explains micro thermal analysis by relating its signals to established parameters of materials, a modulation technique that measures temperature of a probe independent of heating current, and a method that separates sample information from the artifact caused by a measuring probe.

2. Mathematical model

Fig. 1 shows a typical resistive probe used for micro thermal analysis. The probe contains three major parts: conducting wires, a tip and a mirror. Electrical current is passed through the tip to generate required temperature or driving power. The tip possesses much larger resistance than the conducting wire so that heating is concentrated at the tip. The mirror functions as a laser target detecting the deflection of the probe as required by normal AFM functioning.

In analogy to electronic circuit, a probe–sample combination is modeled using thermal circuit as shown in Fig. 2, where the probe is represented by a thermal resistance R_p and capacitance C_p, and the sample is modeled as an effective thermal resistance R_s and capacitance C_s, T is the temperature difference between the tip and ambient temperature and p is the heating power generated at the tip of the probe. The relationship between these parameters

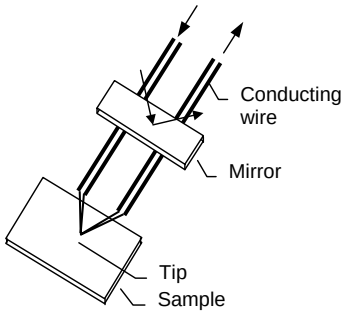

Fig. 1. Thermal probe.

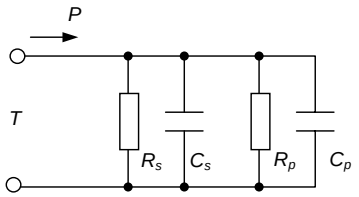

Fig. 2. Modeling of probe–sample combination.

follows

$$p = T\left(\frac{1}{R_\mathrm{p}} + i\omega C_\mathrm{p} + \frac{1}{R_\mathrm{s}} + i\omega C_\mathrm{s}\right) \tag{1}$$

where $i = \sqrt{-1}$, ω is the angular frequency of ac thermal waves. In absence of ac modulation, Eq. (1) is simplified as

$$p = T\left(\frac{1}{R_\mathrm{p}} + \frac{1}{R_\mathrm{s}}\right) \tag{2}$$

If only the sample is considered, the model becomes

$$p_\mathrm{s} = T\left(\frac{1}{R_\mathrm{s}} + i\omega C_\mathrm{s}\right) \tag{3}$$

Since the probe contacts only a small area of a sample, the physical meanings of R_s and C_s are completely different from that of bulk material. This forms the difference in theory between micro and bulk thermal analysis. Interpretation of the two parameters will be focused in the following chapters. All theories are based on well-accepted heat conduction equation,

$$\frac{\partial T}{\partial t} = \kappa \nabla^2 T \tag{4}$$

where κ is thermal diffusivity, the definition of which is known as

$$\kappa = \frac{\lambda}{\rho S} \tag{5}$$

where λ is thermal conductivity, ρ the density and S the specific heat. Heat conduction equation takes different forms in different coordinate system. One and three-dimensional models will be discussed assuming that the sample is homogenous and isotropic.

2.1. One-dimensional model

One-dimensional model assumes that heat transfer inside a sample is limited in z (vertical) direction only. Diffusion in other directions is negligible. Such a model may apply to very thin film where the size of probe is relatively bigger comparing with the thickness of thin film. One-dimensional model is shown in Fig. 3, which can be described mathematically as

$$\frac{\partial T(z,t)}{\partial t} = \kappa \frac{\partial^2 T(z,t)}{\partial z^2} \quad 0 < z < d,\ t > 0 \tag{6}$$

$$T(0,t) = T_\mathrm{A} \mathrm{e}^{i\omega t} \tag{7}$$

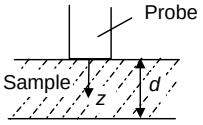

Fig. 3. One-dimensional model.

$$T(d, t) = 0 \tag{8}$$

where d is the thickness of the sample, $T(z, t)$ denotes the temperature of sample at depth z and time t, T_A the amplitude of ac temperature at the probe and ω the angular frequency of thermal waves. Eq. (6) is actually the heat conduction equation written in one-dimensional coordinate, Eqs. (7) and (8) are boundary conditions that define the temperature at the probe, and that on other side of the sample which is equal to ambient temperature. A general solution for Eq. (6) is

$$T(z, t) = \left(A_1 \exp\left(-z(1+i)\sqrt{\frac{\omega}{2\kappa}}\right) + A_2 \exp\left(z(1+i)\sqrt{\frac{\omega}{2\kappa}}\right)\right) \exp(i\omega t) \tag{9}$$

where A_1 and A_2 are coefficients determined by boundary conditions. Denoting

$$\eta = (1+i)\sqrt{\frac{\omega}{2\kappa}} \tag{10}$$

and applying boundary conditions, Eq. (9) becomes

$$T(z, t) = T_A \exp(i\omega t) \frac{\exp(-z\eta) - \exp((-2d+z)\eta)}{1 - \exp(-2d\eta)} \tag{11}$$

The power flow to the sample, according to Fourier's Law of Conduction, is

$$p(0, t) = -\lambda A \left.\frac{dT}{dz}\right|_{z=0} = \lambda A T_A \exp(i\omega t) \coth(d\eta)\eta \tag{12}$$

where A is the contacting area between the probe and sample, λ is the thermal conductivity at measured sample point, and coth denotes hyperbolic cotangent function. Eqs. (11) and (12) are somewhat complicated. Simplification is possible if a sample falls into specified thick or thin sample model in the following.

2.1.1. Thick sample model

Thick sample assumes that a sample is thick enough that majority of heat is absorbed by the sample, rather than passing through it. Thick sample is described mathematically as

$$2d\sqrt{\frac{\omega}{2\kappa}} \gg 1 \quad \text{i.e.} \quad d \gg \sqrt{\frac{\kappa}{2\omega}} \tag{13}$$

Using approximations

$$\exp(-2d\eta) \approx 0 \quad \text{and} \quad \coth(d\eta) \approx 1 \tag{14}$$

Eq. (11) is simplified as

$$T(z, t) = T_A \exp\left(-z\sqrt{\frac{\omega}{2\kappa}}\right) \exp\left(i\left(\omega t - z\sqrt{\frac{\omega}{2\kappa}}\right)\right) \tag{15}$$

and Eq. (12) as

$$p(0, t) = AT(0, t)\sqrt{\frac{\omega\lambda\rho S}{2}}(1+i) \tag{16}$$

From Eq. (15), It is clear that the amplitude of temperature inside a sample decreases as exponential function of z. A special depth at

$$\tau = \sqrt{\frac{2\kappa}{\omega}} \tag{17}$$

designates where the amplitude of temperature attenuates to $1/e$ of the probe temperature. τ is referred to as penetration constant in this paper. It is a function of both diffusivity and frequency. Table 1 lists typical values of penetration constant for a number of materials.

We also find, from Eq. (16), that the phase signal of power is 45°, which cannot be used to measure thermal properties. Comparing Eq. (16) to (3), we obtain

$$\frac{1}{R_s} = A\sqrt{\frac{\omega\lambda\rho S}{2}} \tag{18}$$

$$C_s = A\sqrt{\frac{\lambda\rho S}{2\omega}} \tag{19}$$

where R_s and C_s are the effective thermal resistance and capacitance of sample as seen by the probe. $1/R_s$ will be referred to as thermal conductance.

2.1.2. Thin sample model

Contrary to thick model, thin sample model assumes that a sample is so thin that the majority of heat passes though the

Table 1

Material	λ (W/m K)	S (J/kg K)	ρ (kg/m^3)	κ (m^2/s)	τ (m) @ 200 Hz
Polystyrene (PS)	0.12	1200	1050	9.5E-8	8.7E-6
Polyethylene terephthalate (PET)	0.14	1300	1300	8.3E-8	8.1E-6
Polypropylene (PP)	0.15	1800	900	9.3E-8	8.6E-6
Polymethyl methacrylate (PMMA)	0.18	1450	1190	1.0E-7	9.1E-6
Polyvinyl chloride (PVC)	0.16	1046	1400	1.1E-7	9.3E-6
Polyethlene (PEHD)	0.48	1900	950	2.7E-7	1.5E-5
Platinum	71.6	133	21450	2.5E-5	1.4E-4

sample rather than being absorbed. Thin sample is defined mathematically as

$$2d\sqrt{\frac{\omega}{2\kappa}} \ll 1 \quad \text{i.e.} \quad d \ll \sqrt{\frac{\kappa}{2\omega}} \tag{20}$$

Using approximations

$$\exp(-2d\eta) \approx 1 - 2d\eta, \quad \exp(-2z\eta) \approx 1 - 2z\eta \quad \text{and}$$
$$\coth(d\eta) = \frac{1}{d\eta} + \frac{d\eta}{3} \tag{21}$$

Eq. (11) becomes

$$T(z,t) = T_{\mathrm{A}} \exp(i\omega t)\left(1 - \frac{z}{d}\right) \tag{22}$$

and Eq. (12) becomes

$$p(0,t) = \lambda A T(0,t)\left(\frac{1}{d} + i\frac{d\omega}{3\kappa}\right) \tag{23}$$

It is understandable that temperature distribution, according to Eq. (22), is linear inside a thin sample, and power signal, according to Eq. (23), leads the temperature by a phase that is related to diffusivity. Comparing Eq. (23) to (3), effective thermal conductance and capacity are obtained,

$$\frac{1}{R_{\mathrm{s}}} = \frac{A\lambda}{d} \tag{24}$$

$$C_{\mathrm{s}} = \frac{A\lambda d}{3\kappa} = \frac{Ad\rho S}{3} \tag{25}$$

Obviously, both thick and thin sample models take simpler mathematical forms than the general solution in Eqs. (11) and (12). This simplifies math for analysis. Which model to use, thick or thin, depends on not only the physical thickness of a sample, but also the frequency of modulation. This characteristic makes it possible to fit a sample to either thick or thin model by merely changing modulation frequency other than the physical thickness of a sample. A same sample may fit to thick sample model if the modulation frequency is high enough, or thin sample model if the frequency is low enough.

2.2. Three-dimensional model

Three-dimensional model assumes that heat transfer inside a sample is compatible in all directions. This happens when the size of a probe is significantly smaller than a sample in all directions. Spherical coordinates will be used for the modeling, as shown in Fig. 4. For simplicity in math, the geometry of the tip of a thermal probe is simplified as a hemisphere with a radius of r_{p}. We define r to be the distance (radius) between interested point and the center of the tip and θ to be polar angle from the vertical axis of the hemisphere restricted to $0 \le \theta < \pi/2$. Azimuthal angle is not defined since the geometry of the sample and probe has no dependence on this coordinate. Rewriting heat conduction Eq. (4) in the spherical coordinate, we have

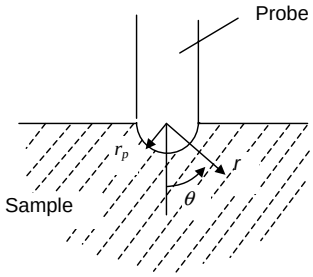

Fig. 4. Three-dimensional model.

$$\frac{\partial T}{\partial t} = \kappa\left(\frac{\partial^2 T}{\partial r^2} + \frac{2\partial T}{r\partial r} + \frac{\cos\theta}{r^2\sin\theta}\frac{\partial T}{\partial \theta} + \frac{\partial^2 T}{r^2\partial\theta^2}\right) \tag{26}$$

where

$$T|_{r=r_{\mathrm{p}}} = T_A \exp(i\omega t) \quad (0 \le \theta < \pi/2) \tag{27}$$

$$T|_{r=r_{\mathrm{s}}} = 0 \quad (0 \le \theta < \pi/2) \tag{28}$$

$$\frac{\partial T}{\partial \theta}|_{\theta=\pi/2} = 0 \tag{29}$$

T denotes the temperature of interested point at radius r, polar angle θ and time t, r_{s} is the outside radius of the sample, T_{A} is the amplitude of ac temperature at the probe, and ω the angular frequency of thermal wave. Eqs. (27)–(29) are boundary conditions, defining that the temperature at the probe is sinusoidal, the temperature at outside radius of the sample $r = r_{\mathrm{s}}$ is zero and that the gradient of temperature at the upper surface of the sample is zero to assert that the sample is thermally isolated from its surroundings aside from the probe tip. Using a conventional technique for solving partial differential equations, we assume

$$T(r,\theta,t) = R(r)F(\theta)U(t) \tag{30}$$

The general solution of $F(\theta)$ can be expressed in Legendre polynomials

$$F(\theta) = \sum_{n=0}^{\infty} c_n P_n(\cos(\theta)) \tag{31}$$

where c_n is the Legendre coefficients, and P_n is the nth Legendre polynomials. Since the temperature T is defined only over the hemisphere, and the even-ordered Legendre polynomials form a complete orthonormal set on that domain, we restrict n to be even in (31); this restriction also satisfies (29). Furthermore, since (27) and (28) have no angular dependence, only the $n = 0$ term from (31) is non-zero. Therefore

$$c_n = 0 \quad (n = 1, 2, 3\ldots) \tag{32}$$

and

$$F(\theta) = c_0 P_0(\cos(\theta)) = c_0 \tag{33}$$

Obviously T has no dependence on θ in the range (0, π/2). Differential Eq. (26) is further rewritten as

$$\frac{\partial T}{\partial t} = \kappa\left(\frac{\partial^2 T}{\partial r^2} + \frac{2\partial T}{r\partial r}\right) \quad 0 \le \theta < \pi/2 \tag{34}$$

A solution for Eq. (34) is

$$T = \left(A_1\frac{1}{r}\exp(-r\eta) + A_2\frac{1}{r}\exp(r\eta)\right)\exp(i\omega t) \tag{35}$$

where η is defined in Eq. (10), A_1 and A_2 are constants determined by boundary conditions. Applying boundary conditions (27) and (28), we have

$$A_1 = \frac{-r_p T_A \exp(2r_s\eta)}{\exp(r_p\mu) - \exp((2r_s - r_p)\eta)} \tag{36}$$

$$A_2 = \frac{r_p T_A}{\exp(r_p\eta) - \exp((2r_s - r_p)\eta)} \tag{37}$$

Substituting A_1 and A_2 in (35), we have

$$T = \frac{r_p T_A \exp(i\omega t)}{r} \times \frac{-\exp((2r_s - r_p - r)\eta) + \exp((r - r_p)\eta)}{1 - \exp(2(r_s - r_p)\eta)} \tag{38}$$

The power flow into the sample, according to Fourier's Law of Conduction, is

$$p(0,t) = -\lambda 2\pi r_p^2 \left.\frac{dT}{dr}\right|_{r=r_p} = \frac{T_A \exp(i\omega t)\lambda 2\pi r_p^2}{1 - \exp(2(r_s - r_p)\eta)} \times \left[-\left(\frac{1}{r_p} + \eta\right)\exp(2(r_s - r_p)\eta) + \left(\frac{1}{r_p} - \eta\right)\right] \tag{39}$$

Eqs. (38) and (39) are general solutions for spherical model. Simpler form will be derived for thick and thin sphere models in the following.

2.2.1. Thick spherical model

Similar to one-dimensional case, thick spherical model assumes a sample is much thicker than penetration constant, i.e.

$$r_s - r_p \gg \sqrt{\frac{2\kappa}{\omega}} \tag{40}$$

In this case, Eq. (38) is simplified as

$$T(r,t) = T_A\frac{r_p}{r}\exp\left(-(r - r_p)\sqrt{\frac{\omega}{2\kappa}}\right) \times \exp\left(i\left(\omega t - (r - r_p)\sqrt{\frac{\omega}{2\kappa}}\right)\right) \tag{41}$$

Obviously two parts contribute to the attenuation of temperature amplitudes inside the sample: an exponential part similar to one-dimensional model and an additional reciprocal part of r. The latter makes the attenuation much faster than one-dimensional model. Heat flow Eq. (39) is simplified as

$$p(r_p,t) = 2\pi r_p^2 \lambda T(r_p,t)\left[\frac{1}{r_p} + (1+i)\sqrt{\frac{\omega}{2\kappa}}\right] \tag{42}$$

Comparing Eq. (42) to (3), the effective thermal conductance and capacity as seen by the probe are obtained,

$$\frac{1}{R_s} = 2\pi r_p^2\lambda\left(\frac{1}{r_p} + \sqrt{\frac{\omega}{2\kappa}}\right) = 2\pi r_p^2\left(\frac{\lambda}{r_p} + \sqrt{\frac{\omega\lambda\rho S}{2}}\right) \tag{43}$$

$$C_s = \frac{2\pi r_p^2\lambda}{\sqrt{2\omega\kappa}} = 2\pi r_p^2\sqrt{\frac{\lambda\rho S}{2\omega}} \tag{44}$$

2.2.2. Thin spherical model

Thin spherical model applies when the thickness of a sample meets the criteria,

$$r_s - r_p \ll \sqrt{\frac{2\kappa}{\omega}} \tag{45}$$

In this case, (38) and (39) are simplified as

$$T = \frac{r_p(r_s - r)}{r(r_s - r_p)}T_A\exp(i\omega t) \tag{46}$$

and

$$p = 2\pi r_p^2\lambda T_A\exp(i\omega t)\left(\frac{1}{r_s - r_p} + \frac{1}{r_p} + i(r_s - r_p)\frac{\omega}{3\kappa}\right) \tag{47}$$

respectively. Comparing Eq. (47) to (3), effective thermal conductance and capacity as seen by the probe are obtained,

$$\frac{1}{R_s} = 2\pi r_p^2\lambda\left(\frac{1}{r_s - r_p} + \frac{1}{r_p}\right) \tag{48}$$

$$C_s = 2\pi r_p^2(r_s - r_p)\frac{\rho S}{3} \tag{49}$$

Similar to one-dimensional model, thick and thin sphere models possess much simpler mathematical form than the general solution. A sample can easily fit to either thick or thin sample model by changing the frequency of modulation.

It should be noted that, although above equations are derived primarily for ac modulation, thin sample models also apply to dc measurements if letting $\omega = 0$ and interpreting the temperature T as the temperature difference between interested point and ambient temperature.

2.3. Removing artifact caused by thermal probes

Experiments show that the power consumed by a typical polymer sample is usually a fraction of what is consumed by a probe. As a result, a typical thermal signal, such as temperature response to ac power modulation, usually contains more artifact from the probe than the real information from the sample. To make meaningful measurements

the artifact must be removed. Two methods are available for this purpose: (1) differential measurement using two probes with one as measuring probe and the other as reference probe, and (2) two-cycle measurement using a single probe with the first cycle performed with the probe not in contact with the sample and the second in normal contact with the sample. Differential method usually provides better cancellation for long haul measurement where ambient conditions may change significantly. Its disadvantage is that it requires two well-balanced reference probes. Two-cycle measurement does not require a reference probe, but introduces noise caused by changes in ambient conditions. It is suitable for measurements that can be done within a short period and/or in a stable environment. Considering the difficulty to manufacture two identical thermal probes and the short time (usually 1–2 min) needed to make a measurement for micro thermal analysis, two-cycle method is preferred. Both cycles can run either same temperature program or same power program. In case of same temperature program, simple subtraction of power signals recorded from two cycles, according to Eq. (1) and (2), is capable of removing probe artifact,

$$p(k) - p'(k) = T(k)\left[\frac{1}{R_s(k)} + i\omega C_s(k)\right] \tag{50}$$

where k is the serious number of measuring points, $p(k)$ and $p'(k)$ are complex powers measured in loaded and no-load cycles respectively. $T(k)$ is the temperature of the kth measuring point which is same in both cycles. Dividing both sides of Eq. (50) by $T(k)$ gives

$$\frac{1}{R_s(k)} + i\omega C_s(k) = \frac{p(k) - p'(k)}{T(k)} \tag{51}$$

In case same power program is run, the artifacts of a probe is removed by the following algorithm,

$$\frac{1}{T(k)} - \frac{1}{T'(k)} = \frac{1/R_s(k) + i\omega C_s(k)}{p(k)} \tag{52}$$

where $T(k)$ and $T'(k)$ are the complex temperature measured in loaded and no-load cycles respectively. $p(k)$ is the power applied to the kth point which is same for both cycles. Multiplying both sides of Eq. (52) by $p(k)$ we have

$$\frac{1}{R_s(k)} + i\omega C_s(k) = \frac{p(k)}{T(k)} - \frac{p(k)}{T'(k)} \tag{53}$$

As mentioned earlier, a practical probe may consumes ten times more power than a polymer sample. The difference of temperature responses between loaded and no-load measurements for same power input is actually very small. In this case, we have

$$\frac{1}{T(k)} - \frac{1}{T'(k)} = \frac{T'(k) - T(k)}{T'(k)T(k)} \approx \frac{T'(k) - T(k)}{T^2(k)} \tag{54}$$

Accordingly, Eq. (52) becomes

$$T'(k) - T(k) \approx \left[\frac{1}{R_s(k)} + i\omega C_s(k)\right]\frac{T^2(k)}{p(k)} \tag{55}$$

Obviously, the difference of temperature responses also provides the needed cancellation of probe artifact as long as the power consumed by the probe is much bigger than the sample.For the convenience of description, $1/R_s + i\omega C_s$ will be referred to as complex conductance, $1/R_s$ and ωC_s as the real and imaginary conductance respectively.

3. Instrumentation

Based on previous analysis, a scanning thermal microscope can either measure power for a known temperature input or measure temperature response for a known power input. In both modes, the artifact caused by a probe can be removed. Power input mode is technically easier to realize, as it does not involve any thermal dynamics of either the probe or the sample. Temperature input mode is easier for user to specify the temperature range, more straight forwards. But it has to take into account thermal dynamics, which make the controller more complicated and less accurate when controlling fast changing ac temperature. To take advantage of both modes, new design adopts temperature input mode for dc measurements, offering the convenience to specify temperature, and power input mode for ac modulation to achieve more accurate control.

Fig. 5 shows the schematic for thermal control. There are three input signals on the left side. The high frequency signal is for temperature measurement. The signal generates constant amplitude of high frequency current in the probe through voltage-to-current converter V/I**.** The amplitude of voltage drop across the probe at this frequency is measured using Lock-in Amplifier 1. Since the current is constant in amplitude, the output from Lock-in Amplifier 1, T, is proportional to probe resistance, or temperature. The dc signal on the left of Fig. 1 is temperature input command. A comparator compares the temperature command to measured dc temperature T_{dc}, obtained after passing temperature signal T through a low pass filter LPF. The error signal generated by the comparator is then transmitted to a controller, which in turn generates a voltage signal that will ultimately be applied to the probe as a current, according to the value and sign of the error signal, to cause the dc temperature of the probe to follow the command temperature. The power consumption of probe P is measured by multiplying the voltage drop across the probe by its current. DC power, P_{dc}, corresponding to dc temperature command is obtained by passing power signal P through low-pass filter LPF1. The low frequency signal on the left is the ac power modulation input. The signal is first combined with the output from the controller, then transmitted to a square root electronic, and finally generates a current in the probe through voltage-to-current converter V/I,

$$I = \sqrt{G(V_c + V_1 \cos \omega t)} \tag{56}$$

where V_c is the output voltage from the controller, the value of which depends on dc power required to maintain or raise

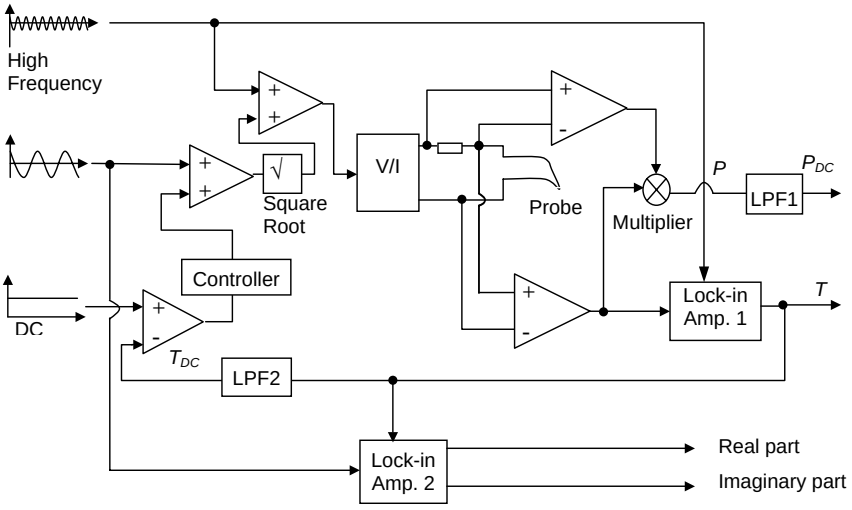

Fig. 5. Schematic of measuring electronics.

the DC temperature, $V_1 \cos \omega t$ is the low frequency input for power modulation and G is the gain of voltage to current converter V/I. The power generated in the probe is

$$p = I^2 R_p = G(V_c + V_1 \cos \omega t) R_p \quad (57)$$

where R_p is the resistance of thermal probe. Since the amplitude of power modulation is usually very small (typically a few degrees), the variation of R_p within an ac modulation cycle is negligible. The variation of resistance resulted from dc heating is a slow process, the impact of which is compensated by software. Ac temperature response is measured by lock-in amplifier 2, which generates two outputs: the real and imaginary parts of ac temperature. The physical meaning of real part is the component of temperature having same phase as ac power input, and the imaginary part having a phase leading ac power by 90°. Real and imaginary components of temperature form a complex number, which is referred to as the complex ac temperature and cited in equations from (52) to (55).

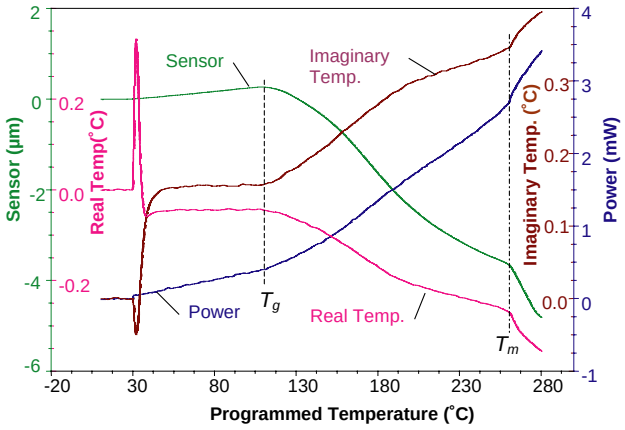

Fig. 6. Polyethylene terephthalate (PET) sample.

4. Experiments

Practical measurements of some polymers were conducted using Veeco "Explorer" AFM. Wollaston wire probe is used as the measuring probe. High frequency current for temperature measurement is operated at 100 kHz. Typical amplitude for ac power modulation ranges from 0.05 to 0.5 mW, generating amplitude of 1–10 °C in temperature for typical polymer samples. Dc temperature ramping rate is typically from 60 to 1500 °C per minute. Frequency for ac modulation ranges from 50 Hz to 1 kHz. The lower frequency boundary is limited by the fast ramping rate of dc temperature since ac signals have to achieve equilibrium before any significant change in dc temperature occurs. The higher boundary is limited by the bandwidth of Wollaston wire probe, which is estimated to be about 0.5–1 kHz. Two-cycle measurements with a single probe are used to remove the artifact caused by the probe. Figs. 6 to 8 show measured results for polyethylene terephthalate

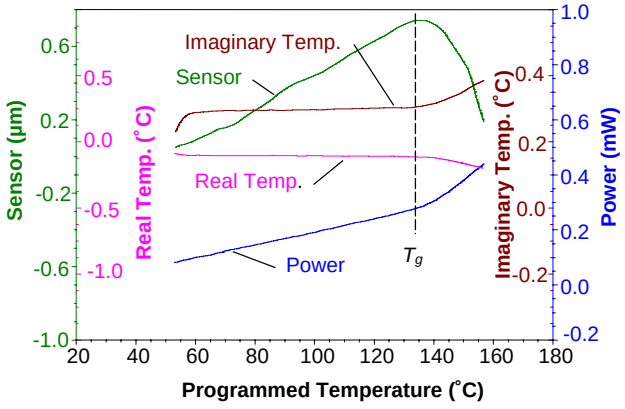

Fig. 7. Polystyrene sample.

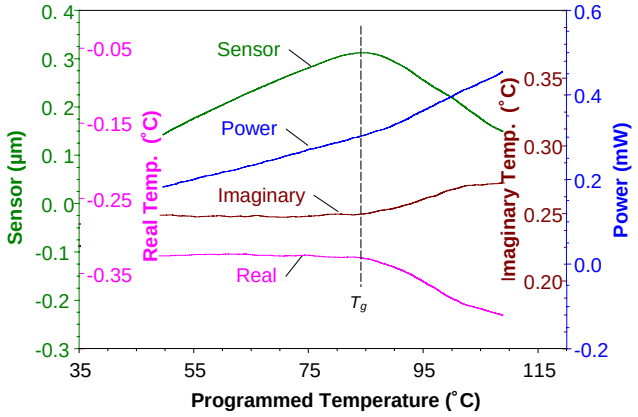

Fig. 8. Polyvinyl chloride (PVC) sample.

(PET), polystyrene and polyvinyl chloride (PVC), respectively. Ac signals are displayed as temperature difference of no load and loaded measurements. In addition to ac signals, dc power and *z*-sensor signal are also displayed for comparison purpose. In either figure the glass transition can be easily identified from ac signals. Ac signals usually exhibit sharper change at glass transition than dc signals. It is also found that glass transitions measured from ac signals are usually a few degrees lower than sensor signal. Since mechanical signal is the response of thermal excitation, the temperature difference is not surprising for fast temperature ramping.

5. Discussion

A theory for micro thermal analysis is briefly introduced. It is based on well-accepted heat conduction equation. One and three-dimensional models are discussed with simplified results for thin and thick sample models. In all models the sample is described using complex conductance, which is in turn related to established parameters of materials, such as thermal conductivity, specific heat and density. Complex conductance is related to not only physical parameters of a sample, but also the modulation frequency. By changing modulation frequency, a sample can usually match either thin or thick sample models.

The introduction of high frequency modulation makes it possible to measure probe temperature independent of heating current. This method measures the first harmonic of temperature instead of the third. It possesses much higher sensitivity than 3-ω method. One benefit of the technique is that we are able to measure ac temperature directly for a known ac power modulation. As power modulation can be done more accurately than temperature modulation, this mode greatly improves the sensitivity of ac measurements. Another benefit is that sample information can be separated from the artifact of the probe for power modulation mode, making it easier to identify phase transitions of polymers through ac signals.

Acknowledgements

The author would like to thank Dr. J. Zadrozny of Veeco Instruments for his input of equations from (29) to (33), Dr. M. Reading of Loughborough University, Dr. A. Hammiche and Dr. H. Pollock of Lancaster University and Dr. G. Slough of TA Instruments for their help in providing background information of earlier technology, discussion over the mathematical model and test of the new design, and Dr. S. Magonov of Veeco Instruments for his samples tested.

References

[1] A. Majumdar, P.C. Carrejo, J. Lai, Appl. Phys. Lett. 62 (1993) 2501.
[2] R.B. Dinwiddie, R.J. Pylkki, P.E. West, Thermal Conductivity 22 (1994) 668.
[3] A. Hammiche, M. Reading, H.M. Pollock, M. Song, D.J. Hourston, Rev. Sci. Instrum. 67 (1996) 4268.
[4] V.V. Gorbunov, N. Fuchigami, V.V. Tsukruk, Probe Microsc. 2 (2000) 53.
[5] V.V. Gorbunov, N. Fuchigami, V.V. Tsukruk, Probe Microsc. 2 (2000) 65.
[6] R. Smallwood, P. Metherall, D. Hose, M. Delves, H. Pollark, A. Hammiche, C. Hodges, V. Mathot, P. Willcocks, Thermochim. Acta 385 (2002) 19.
[7] F. Depasse, P. Grossel, S. Gomes, J. Phys. D Appl. Phys. 36 (2003) 204.
[8] A.I. Buzzin, P. Kamasa, M. Pyda, B. Wunderlich, Thermochim. Acta 381 (2002) 9.
[9] D.Q.M. Craig, V.L. Kett, C.S. Andrews, P.G. Royall, J. Pharma. Sci. 91 (2002) 1201.
[10] D.B. Grandy, D.J. Hourston, D.M. Price, M. Reading, G. Silva, M. Song, P.A. Sykes, Macromolecules 33 (2000) 9348.
[11] D.M. Price, M. Reading, A. Hammiche, H.M. Pollock, Int. J. Pharma. 192 (1999) 85.
[12] S. Lefevre, S. Volz, J.B. Saulnier, C. Fuentes, N. Trannoy, Rev. Sci. Instrum. 74 (2003) 2418.
[13] S. Gomes, F. Depasse, P. Grossel, J. Phys. D Appl. Phys. 31 (1998) 2377.
[14] D.M. Price, M. Reading, A. Caswell, H.M. Pollock, A. Hammiche, Microsc. Anal. 65 (1998) 17.
[15] D. Fryer, R.D. Peters, E.J. Kim, J.E. Tomaszewski, J.J. Pablo, P.F. Nealey, C.C. White, W. Wu, Macromolecules 34 (2001) 5627.
[16] H.M. Pollock, A Hammiche, J. Phys. D Appl. Phys. 34 (2001) R23.
[17] A. Hammiche, L. Bozec, M. Conroy, H.M. Pollock, G. Mills, J.M.R. Weaver, D.M. Price, M. Reading, D.J. Hourston, M. Song, J. Vac. Sci. Technol. B 18 (2000) 1322.
[18] A. Hammiche, D.J. Hourston, H.M. Pollock, M. Reading, M. Song, J. Vac. Sci. Technol. B 14 (1996) 1486.
[19] G. Mills, J.M.R. Weaver, G. Harris, W. Chen, J. Carrejo, L. Johnson, B. Rogers, Ultramicroscopy 80 (1999) 7.
[20] F. Oulevey, N.A. Burnham, G. Gremaud, A.J. Kulik, H.M. Pollock, A. Hammiche, M. Reading, M. Song, D.J. Hourston, Polymer 41 (2000) 3087.
[21] P.G. Royall, D.Q.M. Craig, D.B. Grandy, Thermochim. Acta 380 (2001) 165.
[22] P.G. Royall, D.Q.M. Craig, D.M. Price, M. Reading, T.J. Lever, Int. J. Pharma. 192 (1999) 97.
[23] P.G. Royall, V.L. Hill, D.Q.M. Craig, D.M. Price, M. Reading, Pharma. Res. 18 (2001) 294.
[24] H.M. Pollock, A. Hammiche, J. Phys. D Appl. Phys. 34 (2001) 23.

[25] D.M. Price, M. Reading, A. Hammiche, H.M. Pollock, M.G. Branch, Thermochim. Acta 332 (1999) 143.
[26] R.L. Blaine, C.G. Slough, D.M. Price, Proceedings of the 27th Conference of the North American Thermal Analysis Society, 20–22 September 1999, Savannah, Georgia, p. 691.
[27] P.G. Royall, V.L. Kett, C.S. Andrews, D.Q.M. Craig, J. Phys. Chem. B 105 (2001) 7021.
[28] R. Häβler, E.A. Mühlen, Thermochim. Acta 261 (1–2) (2000) 113.
[29] G.H.W. Sanders, C.J. Roberts, A. Danesh, A.J. Murray, D.M. Price, M.C. Davies, S.J.B. Tendler, M.J. Wilkins, J. Microsc. 198 (2000) 77.
[30] V.V. Tsukruk, V.V. Gorbunov, N. Fuchigami, Thermochim. Acta 395 (2003) 151.
[31] W. Xie, J. Liu, C.W.M. Lee, W. Pan, Thermochim. Acta 367–368 (2001) 135.
[32] G.B.M. Fiege, A. Altes, R. Heiderhoff, L. Josef Balk, J. Phys. D Appl. Phys. 32 (1999) L13.